Temporal Progression of Thalamic Plaques in Alzheimer's Disease Transgenic Mice (TAS10, TPM, TASTPM) – Comparison of MRI and µCT

A. Pohlmann[1], F. Alarakhia[2], B. P. Hayes[3], V. Musoko[4], M. J. Perren[5], D. C. Davies[2], and M. F. James[4]

[1]Academic DPU, GlaxoSmithKline R&D Ltd, Cambridge, United Kingdom, [2]Imperial College London, London, United Kingdom, [3]Respiratory CEDD, GlaxoSmithKline R&D Ltd, Stevenage, United Kingdom, [4]Immuno-Inflammation CEDD, GlaxoSmithKline R&D Ltd, Harlow, United Kingdom, [5]Neuroscience CEDD, GlaxoSmithKline R&D Ltd, Harlow, United Kingdom

Introduction: TAS10, TPM, and TASTPM transgenic mice express Alzheimer's disease-associated human proteins ($APP_{K670N,M671L}$, $PS1_{M146V}$ and both transgenes respectively). Co-accumulation of calcium and ferrous iron in some amyloid plaques has been demonstrated bilaterally in the thalamus of TASTPM[1,2] and APPxPS1[3] mice and these pathologies co-localise with MRI-visible T2* hypointensities (THIs). To study THI development and the correlation with calcium deposition (CT-visible) we imaged mice of the three genotypes at different ages, using MRI and µCT combined with automated image segmentation for plaque volumetry.

Materials and Methods: We studied 64 transgenic mice (20 TAS10, 26 TPM, 18 TASTPM, aged 3-23 months) and 10 wild-type mice (aged 22.6 months) ex-vivo. Experiments complied fully with UK ethical and legal requirements. ***MR Imaging.*** Axial T2*-weighted whole brain images were acquired (4.7T Bruker Biospec, Ettlingen, Germany) using a 3D spoiled gradient-echo sequence (TR/TE/FA = 31ms/25ms/15°, resolution = 156µm). ***µCT Imaging.*** Axial images were acquired (Skyscan 1072 micro-CT, Kontich, Belgium) at 60kV, 100µA (×20 magnification, resolution = 13.7µm). ***Analysis.*** On µCT images calcified plaques are hyperintense; hence these images were inverted before analysis (hyperintensities → hypointensities) allowing µCT and MRI data (Fig.1) to be analysed in the same manner. We analysed a brain section defined by the image slices with visible thalamic plaques, together with the two previous and two subsequent slices. The same thresholding-based automated method was used to segment the THIs (Fig.2) in both image types (MRI, µCT). An oval region-of-interest (ROI) enclosing the THI was drawn on the minimum-intensity-projection (mIP, Fig.1); the intensities of normal brain tissue (mean *m*, std σ) in the environment (env) of this ROI (diameters increased by 20%) defined the segmentation threshold as $m_{env} - 2\sigma_{env}$.

Results and Discussion: THIs were absent in wild-type mice. 116 THIs (MRI: 64, µCT: 52), present in 128 transgenic brain images, were automatically segmented; very few required manual correction. The volume of left and right THIs were combined into a total THI volume (V_{THI}). The rate of volume increase with age differed significantly between genotypes ($V_{THI,TAS10}$ >> $V_{THI,TPM}$, $p<0.000001$) but followed a similar trend in MRI and µCT (Fig.3). The development of MRI-visible THIs (linked to accumulation of ferrous iron), a phenomenon restricted to the thalamus, therefore appears to coincide with progressive calcium deposition.
THI volumes in µCT and MRI correlated well (r = 0.89, Fig.4) with the size of plaques in µCT being ~9% of those seen in MRI (regression: y = 0.0872x-0.0009). This translates into a magnification of THIs in T2*-w images to ~2.25× their µCT diameter, in accordance with the fact that iron deposits distort the magnetic field far beyond their actual localization. This effect also enhances the sensitivity of MRI to these deposits, and very small THIs in MRI (< 0.2mm^3, 4 TPM, 1 TASTPM) expectedly did not show in µCT. All other THIs (except one TPM of 0.32 mm^3) were also present in µCT. None of the TPM mice had CT-visible plaques. All CT-visible plaques coincided with MR-visible THIs.

Conclusions: The presented method for volumetry of T2* hypointensities and CT hyperintensities in mouse brains is robust and ensures high reproducibility. THI volumetry showed age-related growth as well as differences in THI size and rate of development between genotypes in broad agreement with the expected amount of amyloid deposition in these mouse models. These genotype-specific age-related changes may shed light on the pathogenesis of Alzheimer's disease. The signal loss observed in T2* data is likely to be the end result of a biological process leading to large "plaque-like" structures in the thalamus. A close connection between the progressing magnetic susceptibility anomalies in the thalamus and their CT-visible counterparts was shown, which further supports the histology[2] of a few THIs that showed they contain amyloid, calcium and ferrous iron. Amyloid deposition is widespread throughout the brain in the transgenic mice investigated, whilst only thalamic plaques are MR- and CT-visible and calcium positive (von Kossa). This suggests that the signal loss is the result of a process unique to the thalamus or connected regions. Further characterization of THIs is necessary and a full histological analysis of the plaques detected in this study is ongoing.

References: [1] H. Barjat et al, *Alzheimer's & Dementia*, 2006, 2(3):S125. [2] S.C. Evans et al, "Pathologies in the Thalamus of TASTPM…", *British Neuroscience Association*, Harrogate, 1-4 April 2007. [3] M. Dhenain et al, *Neurobiol Aging*, in press, DOI: 10.1016/j.neurobiolaging.2007.05.018.

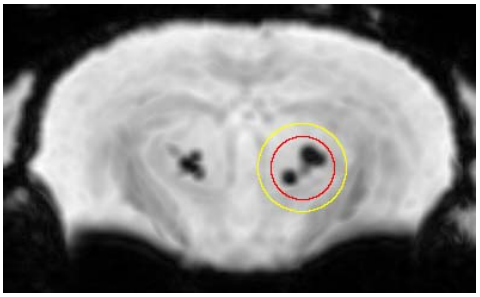

Fig. 1: mIP of a T2*-weighted MRI image stack, showing the THIs with the user defined ROI (red) and the automatically generated environment ROI (yellow).

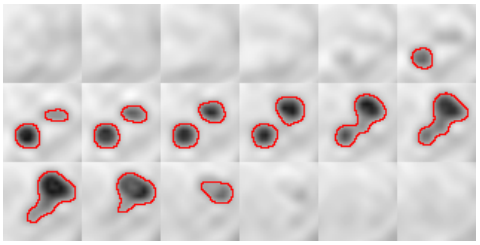

Fig. 2: Montage of 18 MRI image slices (volume of interest only) showing a hypointense (dark) cluster. The red outlines mark the automatically segmented THI voxels.

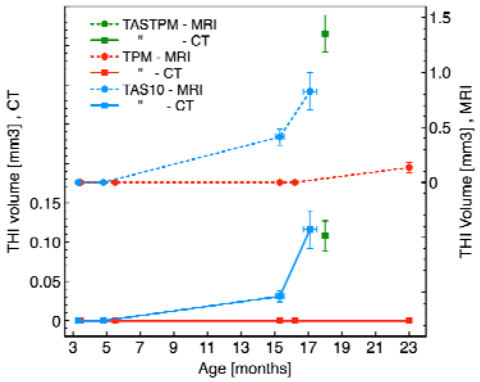

Fig. 3: THI volumes in mm^3 (mean, SEM) versus age. CT-visible thalamic plaques (left axis, lower half of graph) and MRI-visible plaques (right axis, upper half of graph).

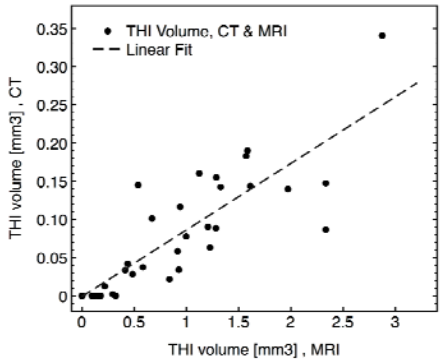

Fig. 4: Correlation of MRI and µCT (r = 0.89). Plot of THI volume in µCT images versus their volume in MRI images.